Original Reaction Sequence of Pb(Yb1/2Nb1/2)O-3-PbTiO3: Consequences on Dielectric Properties and Chemical Order

Charlotte Cochard, Fabienne Karolak, Christine Bogicevic, Orland Guedes, Pierre-Eymeric Janolin

Original reaction sequence of $Pb(Yb_{1/2}Nb_{1/2})O_3$-$PbTiO_3$: consequences on dielectric properties and chemical order

Charlotte Cochard,[1,2] Fabienne Karolak,[1] Christine Bogicevic,[1] Orland Guedes,[2] and Pierre-Eymeric Janolin[1]

[1]*Laboratoire SPMS, Université Paris Saclay, CentraleSupélec, CNRS; Grande voie des vignes, 92295 Chatenay-Malabry, France.*

[2] *Études et Productions Schlumberger, 1 rue H. Becquerel, 92140 Clamart, France*

(Dated: September 12, 2015)

Abstract

The solid-solution $[Pb(Yb_{1/2}Nb_{1/2})O_3]_{1-x}$-$[PbTiO_3]_x$ was synthesized with x≤60%, using several high-temperature techniques as well as room-temperature mechanosynthesis. The high-temperature synthesis reveal a reaction path involving the synthesis first of the end-members before the solid solution. The density and dielectric constant measured on the ceramics prepared from these powders indicate the crucial role of the synthesis technique on the subsequent properties. Mechanosynthesis results in ceramics with higher density and dielectric constant. Identical optimized sintering conditions were then applied to all investigated compositions and the resulting dielectric properties and chemical orders compared. All ferroelectric orders were evidenced. The 1:1 chemical order on the B-site of $Pb(Yb_{1/2}Nb_{1/2})O_3$ results in the formation of a double perovskite Pb_2YbNbO_6, and the superstructures in the X-ray diagrams signing the existence of this order persist up to 30% $PbTiO_3$. The underlying mechanism for substitution of Yb or Nb by Ti is presented.

I. INTRODUCTION

Solid solution between ferroelectric $PbTiO_3$ and perovskites with two elements on the B site (of the general formula $A(BB')O_3$) have attracted considerable interest as they lead to high-performance functional materials such as $Pb(Mg_{1/3},Nb_{2/3})O_3$-$PbTiO_3$[1], $Pb(Zn_{1/3},Nb_{2/3})O_3$-$PbTiO_3$[2], $Pb(Sc_{1/2},Nb_{1/2})O_3$-$PbTiO_3$[3], $Pb(In_{1/2},Nb_{1/2})O_3$-$PbTiO_3$ [4] etc. which are of both fundamental and commercial interests. $Pb(Yb_{1/2}Nb_{1/2})O_3$-$PbTiO_3$ is one of such materials. It exhibits superior high-temperature high-piezoelectric properties, especially at the so-called "morphotropic" phase boundary with a Curie temperature of 370°C (645K) and a piezoelectric coefficient d_{33}~470-510 pC/N[5, 6] which makes it desirable for high-temperature actuators and sensors.

The synthesis of these $A(BB')O_3$ compounds is delicate as pyrochlore phases may easily be formed when all oxides are reacting and are detrimental to the properties. An alternative synthesis route has been designed for $Pb(BB')O_3$ perovskites, the so-called "B-site oxide mixing route"[7, 8] involving the reaction of all oxides but PbO. Depending on the valence of the B-site elements, this leads to the synthesis of a columbite through $B^{2+}O^{2-}+B'^{5+}_2O^{2-}_5 \rightarrow BB'_2O_6$[9] or of a wolframite through $B^{3+}_2O^{2-}_3+B'^{5+}_2O^{2-}_5 \rightarrow 2BB'O_4$ [10] or of a rutile through $B^{4+}O^{2-}_2+B'^{4+}O^{2-}_2 \rightarrow BB'O_4$[11]. In a second step, this columbite, wolframite, or rutile is mixed with PbO to get $Pb(B,B')O_3$. For $Pb(B,B')O_3$-$PbTiO_3$ solid solution, either TiO_2 is added to the other B-site oxides and then PbO is added to the product of this reaction[7, 8] or TiO_2+PbO is added to the wolframite/columbite/rutile[1–4].

In the case of $Pb(B_{1/2}B'_{1/2})O_3$ ferroelectric perovskites, the order on the B site has a dramatic influence on the properties of these materials. Generally speaking, disorder on the B site of the perovskite (i.e. random occupancy by any of the two elements) leads to a relaxor behavior whereas an ordered alternating occupancy of the B site along the [111] direction by the two elements leads generally to antiferroelectric behavior[12]. In the later case, the structure may be described as a "double perovskite" of general formula $Pb_2BB'O_6$. This order doubles the crystallographic unit cell along the [111] direction, giving rise to super-structure X-ray reflections, and was shown to be driven more by the sum of the ionization energies of the two B-site elements rather than by size or charge difference[13]. In the case of $Pb(Yb_{1/2}Nb_{1/2})O_3$ (PYN), the sum of the ionization energies is large (75 eV) leading to a 1:1 chemical order on the B site which could only be broken by adding Lithium to the compound[14].

In this work we investigate three techniques to synthesize $[Pb(Yb_{1/2}Nb_{1/2})O_3]_{1-x}$-$[PbTiO_3]_x$

(PYN-PT) with x≤60% (Ti-richer compositions were considered analogous to $PbTiO_3$) and compare the properties of the ceramics made out of these powders. The investigated techniques are: conventional solid-state mixing, reactive sintering, and mechanosynthesis. An original intermediate reaction step involving the formation of the two end-members is evidenced. The chemical order on the B-site, reminiscent of the one of PYN, is shown to persist in the powders obtained from mechanosynthesis up to composition with 30% $PbTiO_3$.

II. EXPERIMENTAL PROCEDURE

Commercial-grade oxides PbO (Interchim), Yb_2O_3 (Rhône-Poulenc), Nb_2O_5 and TiO_2 (both Alfa Aesar) with purity greater than 99.5% were used as starting materials. Raw materials were mixed in absolute ethanol and subsequently dried in a dry-off oven at 80°C for 24 h before calcination. For every synthesis technique used, the first step consisted in obtaining the $YbNbO_4$ wolframite from the calcination of Yb_2O_3 and Nb_2O_5 at 1200°C for 4 h. For the synthesis of the solid solution, and still for every synthesis techniques, we followed the conventional route, mixing stoichiometric quantities of PbO, TiO_2 and $YbNbO_4$.

For the solid-state technique, we investigated various calcination temperatures and times (800-1000°C and 2-12 h) to get the pure perovskite phase. The reactive sintering technique literally enables to carry out both the synthesis and the sintering of the ceramics from a pellet composed of the reactants[11]. For all compositions investigated, the optimized conditions were 950 to 1050°C for 4 h. For the mechanosynthesis, we used a Retsch mill PM 100, and the pure perovskite phase was obtained after 9 h at 450 rpm. This process takes place at room temperature as the thermal energy of the other techniques is replaced here by mechanical energy.

The X-ray diffraction was carried out on a Bruker D2 phaser to check the crystallinity and purity of the products and on an 18 kW high-precision diffractometer equipped with a rotating Cu anode for the super-structures detection. The X-ray diagrams were either compared with the corresponding JCPDS file (for $PbTiO_3$) or to the literature [15] (for $Pb(Yb_{1/2}Nb_{1/2})O_3$, as no JCPDS file is available) to confirm the perovskite phase and its purity. Scanning Electronic Microscopy (SEM) and Energy Dispersive X-ray spectroscopy (EDX) (Leo Gemini 5130) were performed on fractured samples to investigate the purity and microstructure of the samples. The average grain size were determined using the line interception method on SEM images[16]. The relative density was calculated using geometrical dimension or the Archimedes' method. Dielectric measurements

were carried out using an Agilent 4294A impedance analyzer on ceramics with gold-sputtered electrodes.

III. RESULTS AND DISCUSSION

Starting with the conventional solid-state technique, after 7 h at 950°C, PYN-PT is formed (see Fig.1(a)). However, for shorter calcination times (4 h), extra diffraction peaks related to $Pb(Yb_{1/2}Nb_{1/2})O_3$ and $PbTiO_3$ also appear in Fig.1(b). This suggests that the reaction sequence is actually $PbO+TiO_2+YbNbO_4 \rightarrow Pb(Yb_{1/2}Nb_{1/2})O_3 + PbTiO_3 \rightarrow$PYN-PT. It is highly unusual that the reaction sequence of a solid solution involves forming first the end-members. In order to test whether it is actually possible to synthesize the solid solution from its end members, we synthesized $Pb(Yb_{1/2}Nb_{1/2})O_3$ and $PbTiO_3$ separately, before mixing them and calcining them for 950°C 4 h. We indeed obtained PYN-PT, as can be seen in Fig.1(c). The pyrochlore impurity phase can be eliminated and pure PYN-PT synthesized under optimized synthesis conditions (namely at 800°C for 12 h), see Fig.1(d).

Pyrochlore phases have been shown to form at moderate temperatures (600-700°C) in $Pb(BB')O_3$ and $Pb(BB')O_3$-$PbTiO_3$ solid solutions, even using the B-site mixing route[7, 9, 17, 18] and may still be present in the final product. In PYN-PT, a pyrochlore phase may also be formed but then the end members, PYN and PT, are formed before reacting together to form the PYN-PT solid solution at higher temperature. With optimized synthesis parameters it is possible to obtain pyrochlore-free PYN-PT samples.

The powder of pure perovskite obtained from solid-state synthesis must be shaped and sintered in order to get the final ceramic. As the reaction temperature and the sintering temperature were the same, a more practical solution to prepare ceramics was investigated: reactive sintering. In this case, the raw reactants are pre-pressed into a so-called "green" pellet and both the calcination and sintering occur simultaneously. Following this route we observed the same reaction sequence, i.e. starting from $PbO+YbNbO_4+TiO_2$ leads to the formation of PYN and $PbTiO_3$ and only afterwards of PYN-PT.

In order to prevent the formation of pyrochlore phases, alternative high-pressure and/or high-temperature techniques have been developed, e.g. hot isostatic press. They, however, require heavy equipment. The last technique used to synthesize PYN-PT, mechanosynthesis, was shown to enable the synthesis of pure perovskite phase without such heavy equipment. This room-temperature

technique, also known as ball-milling, was first applied to metallic alloys in the late 70's and to ferroelectric oxides 20 years later[8, 19, 20]. The strain and the grain size reduction taking place during the mechanosynthesis lead to broad and asymmetric peaks in the diffraction patterns making the identification of minority phases in presence difficult. The pure perovskite phase was considered to be obtained when subsequent milling did not change the diffraction pattern. The corresponding X-ray diagram is reported in Fig.1(e) where the large width and asymmetric profile of the peaks associated with the mechanical strain developed in the nanograins can be clearly observed. The difference with the high-temperature synthesis techniques here is that the grain size of the reactants is much smaller (~20 nm vs micro-sized grains) and therefore present a much higher reactivity.

Powders obtained by the solid-state or mechanosynthesis techniques have been sintered (at 950°C for 4 h) and the absence of pyrochlore after sintering was confirmed by X-ray diffraction (not shown). The density and dielectric constant at room temperature of the resulting ceramics are compared with the ceramics obtained by reactive sintering in Table I. The dielectric constants

	d	ϵ'/d
Reactive sintering	60%	302
Solid State reaction+PVA	81%	652
Solid State reaction+1.3%wt PbO	72%	771
Solid State reaction+3%wt PbO	86%	613
Mechanosynthesis	91%	953

TABLE I: Relative density (d) and normalized dielectric constant (ϵ'/d) at room temperature and 1 kHz measured on PYN-PT ceramics with 60% $PbTiO_3$ obtained by the various investigated synthesis techniques. For the solid-state technique, PVA or PbO were used as binders.

reported in Table I have been normalized by the density of the ceramic to enable a meaningful comparison. Because the ceramics prepared from reactive sintering have an extremely low density and therefore open pores, their dielectric constants value cannot be simply compared to the ones of ceramics prepared by the other processing methods. However, it clearly appears that processing ceramics by reactive sintering leads to ceramics of poor quality that are unsuitable for potential applications. The ceramics obtained from mechanosynthesis are the densest and exhibit the highest dielectric constant of all investigated synthesis techniques. A binder was necessary to shape the

powder obtained by the solid-state technique into pellets before sintering. In the case of the first binder used, PVA, SEM and EDX analyses confirmed the absence of carbonated residues after sintering. Addition of PbO instead of PVA was also considered as high-temperature synthesis may lead to Pb evaporation. PbO may also act as a liquid sintering aid. The results are contrasted: if the ceramics density increases with PbO excess compared to reactive sintering, adding 3 wt% excess PbO leads to a normalized dielectric constant lower than with a 1.3 wt% excess PbO. This is because the excess PbO over-compensates for Pb loss during sintering and remains as PbO in the ceramics. Its low dielectric constant (~20) therefore contributes to lower the ceramic dielectric constant.

The influence of the synthesis technique on dielectric properties is presented in Fig.2. Mechanosynthesis leads to the highest dielectric constant at the para-ferroelectric phase transition (T_C ~530°C) with ϵ'_{max}>12 000. The ceramics obtained from solid-state technique exhibit slightly lower ϵ'_{max}, and, as mentioned earlier, excess of PbO decreases ϵ'_{max}. From SEM, we found that even after sintering, the grain size of PYN-PT obtained by mechanosynthesis remains smaller ($\sim 1\,\mu$m) than with other techniques ($\geq 5\,\mu$m). This grain size is close to the optimum grain size giving rise to the best properties. This smaller grain size, combined with strain effects[21], also contribute to lower the transition temperature by ~10°.

Sintering conditions for ceramics obtained by mechanosynthesis were then further optimized with the objective to determine sintering parameters valid over the entire compositional range investigated here (from 0 to 60% $PbTiO_3$). The SEM investigation (Fig.3) reveals that, as expected, the grain size increases with increasing sintering temperature (from 0.086 μm at 800°C for 4 h to 1.27 μm at 1000°C for 4 h) and/or time (from 0.25 μm at 900°C for 2 h to 0.78 μm at 900°C for 6 h). Together with the decrease in the number and size of porosities, this larger grain size lead to an increase of the dielectric constant[1, 4] (Fig.4). At the smallest grain size (0.086 μm), the dielectric peak at the Curie temperature is broad, but still existent indicating the persistence of the ferroelectric properties down to this grain size.

The evolution of the dielectric constant with temperature and the room-temperature diffractograms for selected compositions is presented in Fig.5 and Fig.6, in order to show that antiferroelectric (pure PYN[22, 23] and PYN-5%PT[24, 25]), relaxor (for 25, 30, and 40% $PbTiO_3$ content) and ferroelectric compositions (50 and 60% $PbTiO_3$ content) can be synthesized by this method. Our study focuses on the synthesis of the ceramics, the complete description of their properties together with the type of ferroelectric order they derivate from shall be presented elsewhere.

Fig.6 exhibits super-structure reflections (marked with a square) indicating that the chemical B-site order of PYN persists for PYN-PT compositions with $PbTiO_3$ content up to 30 %. This chemical order reflects an equally probable substitution of Ytterbium and Niobium by Titanium. The details of the microstructural model explaining the origin of these super-structures will be published elsewhere but let us give nevertheless the main idea here. It stems from the strong stability of the Yb/Nb order on the B site of PYN which has been evidenced as an intermediate step in the solid state synthesis technique. Starting from pure PYN, we mentioned before that the chemical formula of this double perovskite may be written Pb_2YbNbO_6 in order to reflect the chemical order existing on the B site along the [111] crystallographic direction. When $PbTiO_3$ is added, Titanium atoms substitute equally each B sites (i.e. Yb or Nb), in order to preserve electroneutrality. This is coherent with the intermediate reaction step observed with high-temperature techniques where the end members are formed before the solid solution. In this scheme, Titanium disturbs a pre-existing order rather than inserts itself in-between Yb/Nb blocks. This situation can be safely rejected as a Yb/Nb/Ti order would lead to a tripling of the unit-cell along [111] and the super-structure reflections would be significantly shifted in the X-ray diagram with respect to their position in PYN. The composition $[Pb(Yb_{1/2}Nb_{1/2})O_3]_{1-x}$-$[PbTiO_3]_x$ may then be written $Pb_2(Yb_{1-x}Ti_x)(Nb_{1-x}Ti_x)O_6$ to reflect the underlying 1:1 chemical order giving rise to the super-structures reported in Fig.6. It is only when there are, on average, more Titanium atoms on the B sites than Ytterbium or Niobium atoms (i.e. for compositions with $PbTiO_3$ content over 33%) that the chemical order is broken and the corresponding super-structures disappear from the X-ray diagram. Such disordered compositions (with Ti content larger than 33%) may be then written $Pb(Yb_{1-x/2},Nb_{1-x/2},Ti_x)O_3$ and the structure of PYN-PT solid solution is described as a simple perovskite.

IV. CONCLUSION

In conclusion we have shown that the end members of the solid solution $Pb(Yb_{1/2}Nb_{1/2})O_3$-$PbTiO_3$ are formed first before the solid solution is obtained in high-temperature synthesis techniques, using the B-site oxides mixing route. Mechanosynthesis was shown to provide a room-temperature alternative to these techniques leading to ceramics with smaller grains but higher dielectric properties and density. Sintering conditions were optimized for all powders with $PbTiO_3$ content up to 60 % and lead to ceramics exhibiting the full diversity of ferroelectric behaviors. From a structural point of view, the so-obtained ceramics exhibit a signature of B-site order remi-

niscent of the PYN one for compositions up to 30 %, that is up to when there is as many Titanium, Ytterbium, and Niobium atoms on the B site of the perovskite.

Acknowledgments

The authors ackowledge the financial support of the ANRT under contract No. 2011/1687.

---

[1] J. Carreaud, P. Gemeiner, J. M. Kiat, B. Dkhil, C. Bogicevic, T. Rojac, and B. Malic. Size-driven relaxation and polar states in $PbMg_{1/3}Nb_{2/3}O_3$-based system. Physical Review B - Condensed Matter and Materials Physics, 72(17):4–9, 2005.

[2] Mouhamed Amin Hentati, Hichem Dammak, Hamadi Khemakhem, and Mai Pham Thi. Dielectric properties and phase transitions of [001], [110], and [111] oriented $Pb(Zn_{1/3}Nb_{2/3})O_3$-6%$PbTiO_3$ single crystals. Journal of Applied Physics, 113(24):–, 2013.

[3] R Haumont, B Dkhil, J M Kiat, A Al-Barakaty, H Dammak, and L Bellaiche. Cationic-competition-induced monoclinic phase in high piezoelectric $(PbSc_{1/2}Nb_{1/2}O_3)_{1-x}$-$(PbTiO_3)_x$ compounds. Phys. Rev. B, 68(1):14114, July 2003.

[4] K. Alilat, M. Pham Thi, H. Dammak, C. Bogicevic, a. Albareda, and M. Doisy. Grain size effect on electromechanical properties and non-linear response of dense nano and microstructured PIN-PT ceramics. Journal of the European Ceramic Society, 30(9):1919–1924, 2010.

[5] T Yamamoto and S Ohashi. Dielectric and Piezoelectric Properties of $Pb(Yb_{1/2}Nb_{1/2})O_3$-$PbTiO_3$ Solid Solution System. Japanese Journal of Applied Physics, 34:5349–5353, 1995.

[6] Jong Bong Lim, Shujun Zhang, and Thomas R Shrout. Relaxor behavior of piezoelectric $Pb(Yb_{1/2}Nb_{1/2})O_3$-$PbTiO_3$ ceramics sintered at low temperature. Journal of Electroceramics, 26(1-4):68–73, February 2011.

[7] Masahiro Orita, Hironobu Satoh, Kazuhiro Aizawa, and Kohei Ametani. Preparation of Ferroelectric Relaxor $Pb(Zn_{1/2}Nb_{2/3})O_3$-$Pb(Mg_{1/3}Nb_{2/3})O_3$-$PbTiO_3$ by Two-Step Calcination Method. Japanese Journal of Applied Physics, 31(Part 1, No. 9B):3261–3264, 1992.

[8] Radhika M. V. Rao, Arvind Halliyal, and Arun M. Umarji. Perovskite Phase Formation in the Relaxor System $[Pb(Fe_{1/2}Nb_{1/2})O_3]_{1-x}$-$[Pb(Zn_{1/3}Nb_{2/3})O_3]_x$. Journal of the American Ceramic Society, 79(1):257–260, 1996.

[9] S.L. Swartz and T.R. Shrout. Fabrication of perovskite lead magnesium niobate. Materials Research Bulletin, 17(10):1245–1250, 1982.

[10] Paul Groves. Fabrication and characterisation of ferroelectric perovskite lead indium niobate. Ferroelectrics, 65(1):67–77, 1985.

[11] Thomas R Shrout, Philippe Papet, Sunuk Kim, and Gye-song Lee. Conventionally Prepared Submicrometer lead-Based Perovskite Powders by Reactive Calcination. 67:1862–1867, 1990.

[12] Charlotte Cochard. Pb($Yb_{1/2}Nb_{1/2}$)O_3-$PbTiO_3$: a model solid solution for the study of polar orders. PhD thesis, Ecole Centrale Paris, 2015.

[13] A A Bokov, N P Protsenko, and Z.-G Ye. Relationship between ionicity, ionic radii and order/disorder in complex perovskites. Journal of Physics and Chemistry of Solids, 61(9):1519–1527, September 2000.

[14] A A Bokov, V Y Shonov, I P Raypevsky, E S Gagarina, and M F Kuprianov. Compositional ordering and phase transitions in Pb($Yb_{0.5}Nb_{0.5}$)O_3. Journal of Physics: Condensed Matter, 5:5491–5504, 1993.

[15] Woong Kil Choo, Jin Kim Kim, Jae Ho Yang, Honn Lim, Jeong Yong Lee, Jeong Rok Kwon, and Chang Hwan Chun. Crystal Structure and B-site Ordering in Antiferroelectric Pb(Mg1/2W1/2)O3, Pb(Co1/2W1/2)O3 and Pb(Yb1/2Nb1/2)O3. Japanese Journal of Applied Physics, 32:4249–4253, 1993.

[16] American Society for Testing and Materials. Standard Test Methods for Determining Average Grain Size.

[17] Yang Zupei, Zhou Shaorong, Qu Shaobo, Cui Bin, and Tian Changsheng. Reaction mechanisms of PMN-PT powder prepared by molten salt synthesis. Ferroelectrics, 265(1):225–232, 2002.

[18] V. V. Bhat, M. V. Radhika Rao, and a. M. Umarji. Dilatometric approach for the determination of the solid state reaction-onset of the lead based relaxor ferroelectric system. Materials Research Bulletin, 38(6):1081–1090, 2003.

[19] Junmin Xue, Dongmei Wan, See-ee Lee, and John Wang. Mechanochemical Synthesis of Lead Zirconate Titanate from Mixed Oxides. Journal of the American Ceramic Society, 92:1687–1692, 1999.

[20] Junmin Xue, John Wang, and Dongmei Wan. Nanosized Barium Titanate Powder by Mechanical Activation. Journal of the American Ceramic Society, 83(1):232–34, 2000.

[21] M. Algueró, J. Ricote, T. Hungría, and a. Castro. High-sensitivity piezoelectric, low-tolerance-factor perovskites by mechanosynthesis. Chemistry of Materials, 19(20):4982–4990, 2007.

[22] Jeong Rok Kwon and Woong Kil Choo. The antiferroelectric crystal structure of the highly ordered complex perovskite $Pb(Yb_{1/2}Nb_{1/2})O_3$. Journal of Physics: Condensed Matter, 3:2147–2155, 1991.

[23] V Demidova, E Gagarina, T Ivanova, and V Sakhnenko. Atomic Structure and Phase Transitions in Antiferroelectric $PbYb_{0.5}Nb_{0.5}O_3$. Ferroelectrics, 159:191–196, 1994.

[24] Hoon Lim, Hyo Jin Kim, and Woong Kil Choo. X-Ray and Dielectric Studies of the Phase Transitions in $Pb(Yb_{1/2}Nb_{1/2})O_3$-$PbTiO_3$ Ceramics. Japanese Journal of Applied Physics, 34(Part 1, No. 9B):5449–5452, sep 1995.

[25] Sang-jin Ahn, Jong-jean Kim, Jai-hyun Kim, and Woong-kil Choo. Nondegenerate hard-mode Raman studies of phase transition in antiferroelectric lead ytterbium niobate-based perovskite compound. journal of Raman Spectroscopy, 37:202–207, 2006.

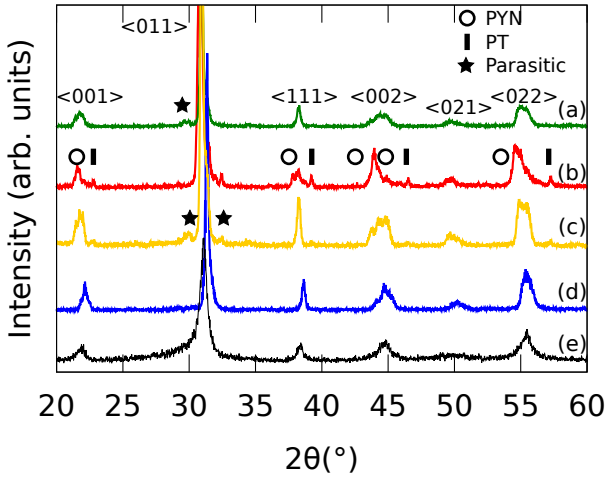

FIG. 1: X-ray diagram of PYN-PT powder (for x=60%) obtained by various techniques : at 950°C by solid-state reaction of $PbO+TiO_2+YbNbO_4$ (a) for 7 h and (b) for shorter calcination time (4 h) revealing the presence of PYN and PT; (c) by solid-state reaction of $Pb(Yb_{1/2}Nb_{1/2})O_3$ + $PbTiO_3$ leading to PYN-PT after 4 h. Pure PYN-PT can be synthesized by solid-state reaction at 800°C for 12 h (d) as well as by mechanosynthesis (e) of $PbO+TiO_2+YbNbO_4$.

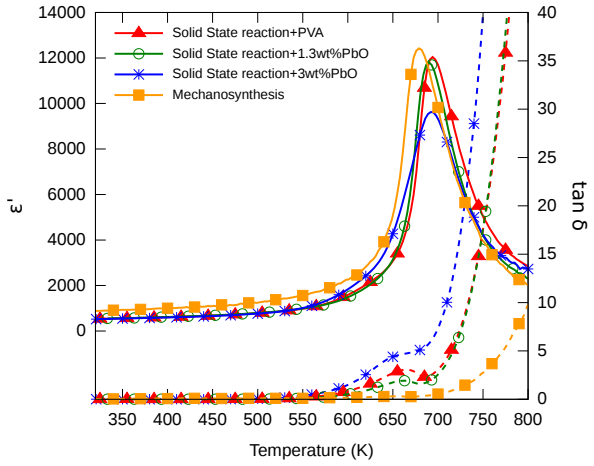

FIG. 2: Real part of the dielectric constant ϵ' (line) and losses tan δ (dotted line) of PYN-PT with 60% $PbTiO_3$ measured at 1 kHz and as a function of temperature on ceramics obtained by various synthesis techniques : +PVA, +1 wt%PbO, +3 wt%PbO designate the binder used with powders obtained by the solid-state technique.

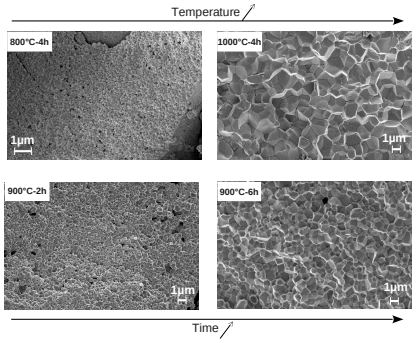

FIG. 3: SEM images of PYN-PT 60% ceramics obtained after sintering at various temperatures and times

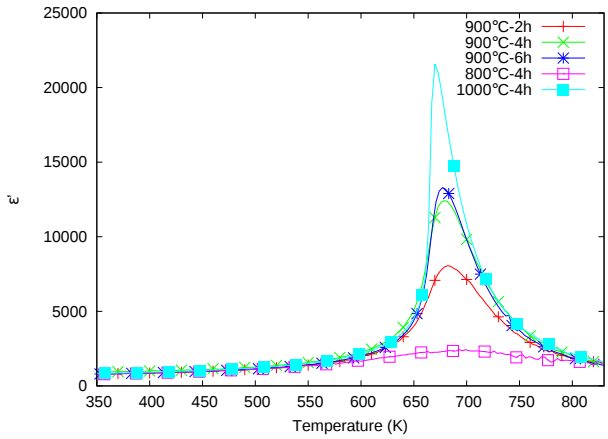

FIG. 4: Real part of the dielectric constant (ϵ') measured at 1 kHz from RT to 530°C of PYN-PT 60% ceramic obtained from various sintering temperature and time.

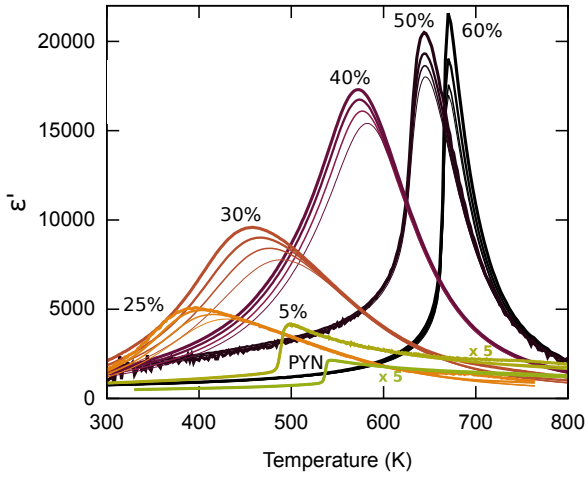

FIG. 5: Real part of the dielectric constant (ϵ') measured at 1 kHz from RT to 530°C on PYN-PT ceramics exhibiting antiferroelectric (pure PYN and PYN-5%PT), relaxor (for 25, 30, and 40% $PbTiO_3$ content) or ferroelectric (50 and 60% $PbTiO_3$ content) behaviors.

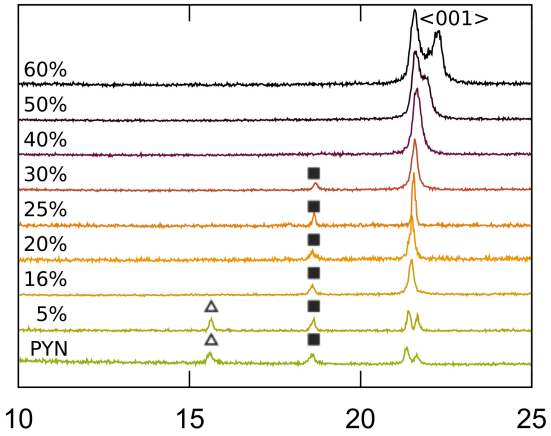

FIG. 6: X-ray diagrams for PYN-PT ceramics obtained by mechanosynthesis for $PbTiO_3$ content between 0 (PYN) and 60 %. Squares (■) indicate super-structure reflections due to chemical order on the B site. Triangles (△) mark super-structures due to antiparallel displacements.